International Journal of Chronic Obstructive Pulmonary Disease Dovepress
open access to scientific and medical research

Open Access Full Text Article ORIGINAL RESEARCH

The Bufei Jianpi Formula Improves Mucosal Immune Function by Remodeling Gut Microbiota Through the SCFAs/GPR43/NLRP3 Pathway in Chronic Obstructive Pulmonary Disease Rats

Jing Mao[1,*], Ya Li[2–4,*], Qingqing Bian[3], Yinshuang Xuan[3], Jingmei Li[3], Zhikun Wang[3], Suxiang Feng[1,2,4], Xuefang Liu[2,4], Yange Tian[2,4], Suyun Li[2–4]

[1]College of Pharmacy, Henan University of Chinese Medicine, Zhengzhou, People's Republic of China; [2]Henan Key Laboratory of Chinese Medicine for Respiratory Disease, Henan University of Chinese Medicine, Zhengzhou, People's Republic of China; [3]Institute for Respiratory Diseases, The First Affiliated Hospital, Henan University of Chinese Medicine, Zhengzhou, People's Republic of China; [4]Co-Construction Collaborative Innovation Center for Chinese Medicine and Respiratory Disease by Henan & Education Ministry of P.R. China, Henan University of Chinese Medicine, Zhengzhou, People's Republic of China

*These authors contributed equally to this work

Correspondence: Suyun Li, Email lisuyun2000@126.com

Purpose: Bufei Jianpi formula (BJF), a traditional Chinese medicine, is an effective and safe therapeutic formula for chronic obstructive pulmonary disease (COPD). BJF treatment is known to reduce the incidence of loose stools in rats with COPD. It is unclear whether BJF regulates gut microbiota. This study examined whether BJF improved mucosal immune function by remodeling the gut microbiota and modulating metabolites in COPD rats.

Methods: Sixty Sprague Dawley (SD) rats were randomized into control, model, BJF, aminophylline (APL), and probiotics (PBT) groups. The stable COPD rat model was duplicated using repeated cigarette smoke inhalation and lipopolysaccharide (LPS) injection. Normal saline, BJF, APL, or PBT were intragastrically administered from weeks eight to twelve, and then the rats were sacrificed at week thirteen. Lung and colon tissues were removed; feces were collected. Pulmonary function, histopathology, levels of inflammatory factors, and activation of NF-κB in the lung tissues were evaluated. Gut microbiota were analyzed using 16S rRNA gene sequencing; fecal short-chain fatty acid (SCFA) concentrations were determined using gas chromatography/mass spectrometry. Mucosal immune response-related genes and proteins were determined using quantitative polymerase chain reaction and Western blotting.

Results: BJF improved pulmonary function and reduced lung inflammation. Further, BJF treatment altered the gut microbiota composition and significantly increased the abundance of Firmicutes and the ratio of Firmicutes to Bacteroides, raising SCFA levels, including acetate, butyrate, and propionate levels. However, the abundance of Bacteroidetes, Proteobacteria, Spirochaetes, Clostridiaceae, and Treponema decreased after BJF administration. BJF decreased the gene and protein expression of NLRP3, Caspase-1, IL-8, and IL-1β, and increased GPR43 expression.

Conclusion: Overall, BJF administration improved mucosal immune function by remodeling the gut microbiota and suppressing the SCFAs/GPR43/NLRP3 pathway in COPD rats. This study provides evidence for the mechanisms underlying BJF-induced improvements in COPD and supports clinical application of BJF.

Keywords: Bufei Jianpi formula, chronic obstructive pulmonary disease, gut microbiota, gut-lung axis, short-chain fatty acids, mucosal immune function

Introduction

Chronic obstructive pulmonary disease (COPD) is the third leading cause of death worldwide and manifests as persistent lung inflammation. Currently, effective treatment methods for COPD are lacking.[1] Although COPD ranks seventh among the

Received: 21 January 2022
Accepted: 22 May 2022
Published: 1 June 2022

leading causes of disability-adjusted life years, it is expected to become the fourth leading cause by 2030, considering its major disease burden on patients' livelihood.[2] Notably, increasing evidence indicates that alterations in the gut microbiome play a significant role in COPD pathogenesis.[3–5] Specifically, clinical data have shown that the gut microbes of patients with COPD were altered compared with those of the healthy population, including decreased alpha diversity and abundance, decreased levels of normal symbiotic bacteria, and increased levels of harmful bacteria (such as *Clostridium* and *Escherichia*).[6] In addition, the gut-lung axis theory indicates that gut microbiome alterations can promote COPD initiation and development by affecting mucosal immunity.[7,8] This has somewhat revealed the connotation of the mucosal immune mechanism, which dictates that "the lungs and large intestines are interior-exteriorly related." Therefore, maintaining gut microbiome homeostasis has provided new insights into the pathophysiology of COPD.

When the gut microbiome is imbalanced, short-chain fatty acids (SCFAs), the most important metabolites of the gut microbiome, diminish. This activates the SCFAs/GPR43/NLRP3 signaling pathway, which plays a key role in the process of gut mucosal immunity.[9] The combination of SCFAs with the free fatty acid receptor GPR43 in gut epithelial cells can stimulate the flow of potassium ions. This, in turn, hyperpolarizes the formation of gut epithelial cell membranes, thus activating NLRP3 inflammasomes. Recruitment of these inflammasomes subsequently activates caspase-1 and promotes the maturation and secretion of pro-IL-1β and pro-IL-8, thereby triggering the body's anti-pathogenic immune inflammatory responses.[10] This compromises the immune function of the respiratory tract mucosa, which aggravates COPD progression. Thus, improving the immune function of the gut mucosa and restoring gut microbiome homeostasis may be an effective treatment strategy for COPD.

The Bufei Jianpi Formula, a traditional Chinese medicine, comprises twelve herbs including *Codonopsis pilosula* (Franch.) Nannf, *Astragalus mongholicus* Bunge, *Atractylodes macrocephala* Koidz, *Poria cocos* (Schw.) Wolf, *Polygonatum kingianum* Collett & Hemsl, *Fritillaria thunbergii* Miq, *Pheretima aspergillum* (E.Perrier), *Magnolia officinalis* Rehder & E.H.Wilson, *Citrus reticulata* Blanco, *Aster tataricus* L.f., *Epimedium brevicomu Maxim*, and *Ardisia japonica* (Thunb.) Blume. Recent evidence indicates that Astragalus polysaccharides (APS) effectively improve gut microbial structure and function in high-fat-diet-fed mice.[11] Our previous studies have demonstrated that BJF alleviates COPD symptoms, reducing the incidence of loose stools and fatigue and improving pulmonary function, skeletal muscle tension, and tolerance in COPD rats.[12,13] However, there is insufficient research on the effect of BJF on gut microbial structure and the metabolome during the stable phase of COPD. Therefore, this study aimed to determine whether BJF could alleviate COPD by improving the gut microbiome and enhancing mucosal immune function through regulation of microbiome structure and function. The results of this study shed light on the gut microecology of COPD, reveal the mechanism of action of BJF in COPD treatment, and identify drug target molecules for COPD management.

Materials and Methods

Animals and Induction of the COPD Rat Model

Sixty Sprague Dawley (SD) rats (200 ± 20 g) were purchased from SPF Biotechnology Co., Ltd. (Shandong, China). The rats were housed in the animal facilities at 25 ± 2°C, 50 ± 10% relative humidity, and a 12 h light/dark cycle for 1 week prior to the experiment. They had ad libitum access to standard food and water.

The COPD rat model was prepared as described previously.[14,15] Briefly, the SD rats were exposed to tobacco smoke (Hongqi Canal® Filter cigarettes, Henan Tobacco Industry, Zhengzhou, China; each cigarette contained 10 mg tar oil, 1.0 mg nicotine and 12 mg carbon monoxide) from a smoke generator (BUXCO, Wilmington, NC, USA) 30 min per exposure (concentration: 3000± 500 ppm), twice a day, with three hour smoke-free intervals, from week one through week eight. In addition, the LPS (1 mg/kg) purchased from Sigma-Aldrich Co., Ltd. was slowly dropped into the nasal cavities of rats, twice per week for the first eight weeks. The control rats were administered 0.9% saline (0.2 mL).

BJF Preparation

BJF was prepared as a dry extract, as described previously.[16] The BJF sample for HPLC-MS analysis was prepared as described previously.[17] The masses of the main active ingredients, bergenin, calycosin-7-glucoside, hesperidin, epimedium A, icariin, nobiletin, and baohuosid I per 1 g of BJF were 1.3456 mg, 0.5616 mg, 1.1755 mg, 0.6869 mg, 1.1195 mg, 0.0951 mg, and 0.0806 mg, respectively.[17]

Experimental Design

To investigate the therapeutic effects of BJF on COPD, the rats were randomly divided into five groups (n = 12 per group): Control, Model, Aminophylline (APL), Probiotics (PBT) and BJF. From weeks eight to twelve, rats in the control and model groups were intragastrically administered normal saline (2 mL), while the other groups were orally administered Aminophylline (27 mg/kg/d, Shandong Xinhua Pharmaceutical Co., Ltd), Probiotics (0.9×10^{10}CFU/kg/d, Pure Encasulations), or BJF (12.42 g/kg/d). Body weights were measured every week throughout the study. At week thirteen, all rats were euthanized by intraperitoneal injection with 150 mg/kg sodium pentobarbital and lung tissue, colon tissue, and fecal samples collected. The equivalent doses of BJF, PBT, and APL were calculated using the formula: D rat = D human × (I rat/I human) × (W rat/W human) 2/3, where D = dose, I = body shape index, and W = body weight.

Pulmonary Function

The forced expiratory vital capacity (FVC), forced expiratory volume in 0.3 s (FEV0.3), and FEV0.3/FVC were measured using a FinePoint™ Pulmonary Function Test system (Buxco Inc., DSI, St. Paul, MN, USA) after the rats were anesthetized and a tracheal cannula was inserted, prior to sacrifice.

Lung and Colon Histopathology

After euthanasia, the rats' left lower lobe of the lung and colon tissues were immediately removed and fixed in 10% neutral buffered formalin solution, embedded in paraffin, cut into 4-mm sections, and stained with Mayer's haematoxylin-eosin (H&E). In addition, colon tissues were stained with H&E and Periodic Acid-Schiff (PAS) to visualize the goblet cells and extent of colonic inflammation. The histopathological changes of the lung and colon tissues in the sections were viewed using an OLYMPUS-DP70 microscope (Olympus, Tokyo, Japan).

Enzyme-Linked Immunosorbent Assay

Frozen lung tissues were weighed and then homogenized on an ice surface. Homogenate was obtained by centrifugation at 1000 g and 4°C for 20 min. The TNF-α, IL-6 and IL-10 levels of lung homogenate were measured with ELISA kits (Elabscience Biotechnology Co., Ltd, Wuhan, China) according to the manufacturer's instructions. TNF-α, IL-6 and IL-10 levels were determined by measuring the absorbance using a microplate reader and plotting a standard curve.

Immunohistochemistry Assay

Lung tissues were embedded in paraffin and cut into 4-μm-thick sections. Tissue slices were blocked with 3% H_2O_2 for 15 min, and 5% bovine serum albumin solution was added. Slides were then incubated with an anti-TNF-α antibody, anti-IL-6 antibody, and anti-IL-10 antibody (GeneTex, CA, USA) at 4 °C overnight, and then with horseradish peroxidase-conjugated secondary antibodies for 30 min, then stained with a DAB solution (Solarbio, Beijing, China). Images were collected for semi-quantitative analysis by Image-Pro Plus 6.0 (Media Cybernetics, Rockville, MD, United States).

NF-κB Activity Assay

NF-κB DNA binding activity was measured using TransAM™ NF-κB p65 Transcription Factor Assay kits (Active Motif, CA, USA) following the manufacturer's instructions. An oligonucleotide containing the NF-κB consensus site (5, -GGGACTTTCC-3,) was loaded into multi-well plates. Then, 20 μL nuclear protein extracted from lung tissues were incubated with 30 μL of binding buffer in microwells coated with the probes containing the NFκB binding consensus. After a 1 h incubation at room temperature with mild agitation, microwells were washed three times. 100 μL of diluted NF-κB antibody (1:1000 dilution) was added to each well and incubated for 1 h. Then, samples were incubated with the secondary antibody (1:1000 dilution) for 1 h at room temperature. Subsequently, optical density was read at 450 nm, using a 655 nm reference wavelength before the colorimetric reaction. The results are expressed after subtraction of the blank values.

Secretory IgA (SIgA) Assay

The colon tissues were longitudinally cut open, then rinsed with sterile alkaline phosphate buffer (PBS) solution (pH7.4). The mucosal surface was gently scraped and mucus placed in an Eppendorf tube containing 0.5 mL sterile PBS (20 mmol/L) and mixed vigorously. After centrifugation (12,000 r/min, 10 min), the supernatant was stored at −80°C. The SigA levels were determined by the SIgA ELISA kits (Elabscience Biotechnology Co., Ltd, Wuhan, China) following the manufacturer's protocol.

Fecal Sample Collection and 16S rRNA Gene Sequencing Analysis

Fecal samples were collected in individual sterile tubes from the rectum of each rat after sacrifice, frozen immediately after sampling and stored at −80°C. Microbial genomic DNA from fecal samples was extracted using a QIAamp DNA Stool Mini Kit (Qiagen, Dusseldorf, Germany) following the manufacturer's instructions. To ensure successful DNA isolation, the DNA was quantified using a NanoDrop instrument (Thermo Fisher Scientific, Waltham, MA, USA). The V3–V4 regions of the 16S rRNA gene were amplified using specific primers (338F 5-ACTCCTACGGGAGGCAGCA-3) and (806R 5′-GGACTACHVGGGTWTCTAAT −3′). The 16S rRNA gene amplicon and sequencing were performed as previously described.[18] 16S rRNA gene sequencing analysis was performed using QIIME (Quantitative Insights Into Microbial Ecology, v1.8.0, http://qiime.org/) and the R package 3.5.1 (https://www.r-project.org/). Chao1 and Shannon indices were used to express the microbial species richness and alpha diversity. Bacterial taxa within different groups were arranged based on relative abundance (false discovery rate < 0.05).

Fecal Short-Chain Fatty Acids (SCFAs)

Fecal SCFA concentrations were measured by gas chromatography/mass spectrometry. 20 mg of fecal samples were placed in a 2 mL microcentrifuge tube. Phosphoric acid (1 mL,0.5% v/v) and a small steel ball were added to the tube. After grinding three times for 10s each, the mixture was vortexed for 10 min and ultrasonicated for 5 min. The mixture was centrifuged at 12,000 rpm for 10 min at 4°C and 0.1 mL of the supernatant was added to a 1.5 mL centrifuge tube. 0.5 mL methyl tert-butyl ether (MTBE) solution was added to the centrifuge tube. The mixture was vortexed for 3 min and ultrasonicated for 5 min, then centrifuged at 12,000 rpm for 10 min at 4°C, and measured by gas chromatography/mass spectrometry (GC/MS) using an Agilent7890B-7000D system (Agilent Technologies, CA, USA). Acetate, propionate, and butyrate were quantified using pure standards diluted in diethyl ether.

Quantitative Real-Time PCR

Total RNA was extracted from colon tissue using a total RNA isolation kit (Solarbio Tech Co., Ltd., Beijing, China) following the manufacturer's instructions, then reverse-transcribed into cDNA using HiScript II reverse transcriptase (EVazyme Biotech Co., Ltd., Nanjing, China). The qPCR primers were designed and synthesized (Genscript, Nanjing, China). The forward and reverse sequences are shown in Table 1. Quantitative real-time PCR reactions were performed using Power Up SYBR Green PCR Master Mix on an ABI 7300 HT Real-Time PCR System (Applied Biosystems, Foster City, CA, USA). The expression of the target genes was normalized to that of GAPDH. Relative expression levels are shown as fold changes relative to the control.

Western Blot

Proteins were extracted from colon tissue samples using RIPA lysis buffer (Solarbio life sciences, Beijing, China). After denaturation, the protein extracts were separated by 10% sodium dodecyl sulfate polyacrylamide gel electrophoresis (SDS-PAGE) for 1 h, then transferred to polyvinylidene difluoride (PVDF) membranes (Millipore, MA, USA) for 2 h. PVDF membranes were probed overnight at 4 °C using the corresponding primary antibodies: anti- GPR43, anti-NLRP3, anti-Caspase-1, anti-IL-8 and anti-IL-1β (GeneTex, CA, USA). After washing thrice with Tris-buffered saline, the membranes were incubated at 25 °C for 1 h with the HRP-conjugated secondary antibody. Antibody binding was determined using a chemiluminescence reagent. The membrane was then scanned and analyzed using a Bio-Rad analyzer

Table 1 List of Primers for Real-Time PCR

Gene Name		Sequence 5′-3′
NLRP3	F	CTCACCTCACACTCCTGCTG
	R	AGAACCTCACAGAGCGTCAC
GPR43	F	ATCCTCACGGCCTACATCCT
	R	CGCCAGGGTCAGATTAAGCA
Caspase-1	F	GACCGAGTGGTTCCCTCAAG
	R	GACGTGTACGAGTGGGTGTT
IL-1β	F	AACTGTGAAATAGCAGCTTTCG
	R	CTGTGAGATTTGAAGCTGGATG
IL-8	F	CATTAATATTTAACGATGTGGATGCGTTTC
	R	GCCTACCATCTTTAAACTGCACAAT
GAPDH	F	ACAGCAACAGGGTGGTGGAC
	R	TTTGAGGGTGCAGCGAACTT

(Hercules, CA, USA). The relative amount of target protein was calculated using the gray value ratios of the protein to GAPDH.

Statistical Analysis

All data are expressed as mean ± standard deviation (SD). Statistical differences in multiple-group comparisons were assessed using one-way analysis of variance (ANOVA). The correlations between specific gut microbiota and SIgA levels and SCFA levels were tested using Spearman correlation test. Statistical significance was set at $P < 0.05$.

Results

Effects of BJF on the Respiratory Function and Gut-Lung Axis Histopathology in COPD Model Rats

To verify the effect of BJF in the treatment of COPD, we examined body weight, respiratory function, and lung and colon histopathology in model rats. As shown in Figure 1A, the body weight of the COPD rats was significantly lower than in the control group from week five (Figure 1A, $P < 0.01$). However, the weight loss of COPD rats was effectively reduced after BJF and PBT treatment from week 10, especially in the BJF group ($P < 0.05$, Figure 1A). There was no significant difference between the Model and APL groups (Figure 1A, $P > 0.05$). Therefore, the BJF treatment effectively alleviated the weight loss of CSE and LPS-induced COPD rats.

Compared with the control group, decreases in the invasive lung function parameters FVC, FEV0.3, and FEV0.3/FVC were observed in the COPD rats (Figure 1B–D, $P < 0.05$). However, the BJF, APL and PBT treatments significantly increased the FVC (Figure 1B, $P < 0.05$), the FEV0.3 were lower in the APL group than in the model group (Figure 1C, $P < 0.01$). No significant changes were observed in the FEV0.3/FVC after four weeks of treatment (Figure 1D, $P > 0.05$).

H&E staining was performed to visualize the histopathological changes in the rat lung and colon; the numbers of inflammatory cells and alveolar fractures and fusions were higher in the COPD group lungs. Notably, administration of BJF, APL and PBT ameliorated pulmonary histopathological damage (Figure 1E). H&E staining of colon histopathology revealed more infiltrating cells, fewer goblet cells, and looser intercellular space in the model group than the control group. BJF, APL and PBT treatment significantly decreased inflammatory cell infiltration, and restored the thickness of the muscle layer (Figure 1F). PAS staining of colon tissues showed that colonic goblet cells in the control group were full and round and mucus secretion was abundant. In comparison, the goblet cells atrophied to varying degrees and the number of goblet cells decreased significantly in COPD rats, while BJF, APL and PBT treatment markedly reversed these changes (Figure 1G).

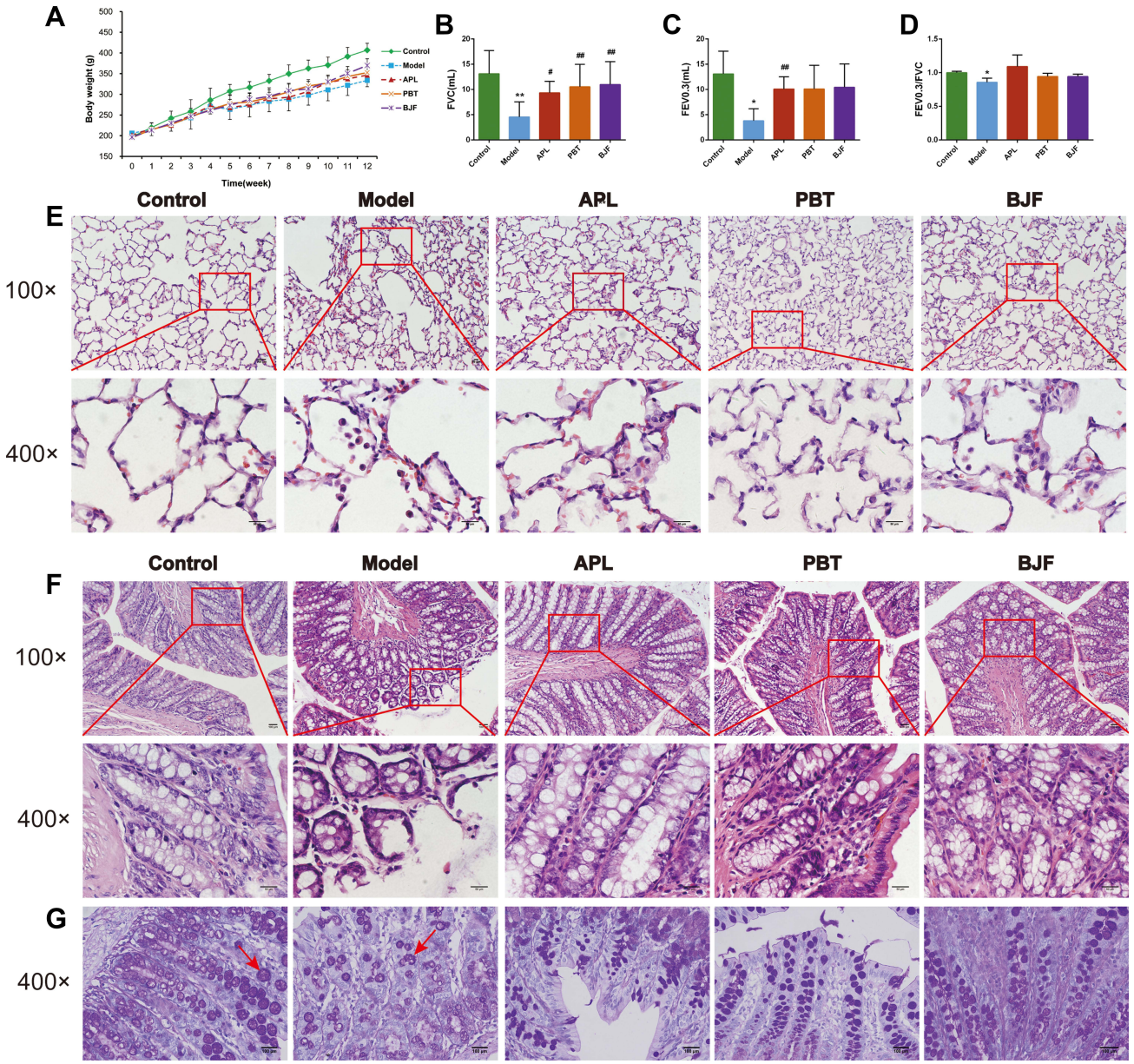

Figure 1 Effects of Bufei Jianpi Formula (BJF) on respiratory function, lung and colon inflammation in COPD model rats. (**A**) Changes in Body weight in each group. (**B–D**) Changes in invasive respiratory function parameters FVC, FEV0.3, and FEV0.3/FVC in each group. (**E**) Histopathological changes of lung tissues in each group (HE staining, magnification, ×100, ×400). (**F**) Histopathological changes of colon tissues in each group (HE staining, magnification, ×100, ×400). (**G**) Histopathological changes of colon tissues in each group (PAS staining, magnification, ×400). Red arrows present the goblet cells. Data are presented as mean ± SD. N = 6 for each group. $^{**}p < 0.01$, $^{*}p < 0.05$ vs control group; $^{\#\#}p < 0.01$, $^{\#}p < 0.05$ vs model group.

Effects of BJF on the Inflammatory Responses in COPD Model Rats

To confirm the effect of BJF on the inflammatory responses, we evaluated the expression levels of inflammatory cytokines in the lung tissue. Compared with the control rats, the levels of TNF-α and IL-6 were higher in the COPD rats (Figure 2A–C, $P < 0.01$), while the level of IL-10 was lower (Figure 2A and D, $P < 0.01$). BJF, APL and PBT treatment significantly inhibited up-regulation of TNF-α and IL-6 in lung tissues, while downregulating IL-10 (Figure 2A–D, $P < 0.01$). Plainly, BJF contributed to alleviating pulmonary inflammatory responses in COPD rats.

Compared with the control group, the TNF-α and IL-6 levels in COPD rats were markedly up-regulated. This alteration was restored by administration of BJF, APL and PBT (Figure 2E and F, $P < 0.01$). IL-10 was rapidly down-regulated in the model group, and increased in lung tissue after BJF, APL and PBT treatment, especially BJF treatment (Figure 2G, $P < 0.01$).

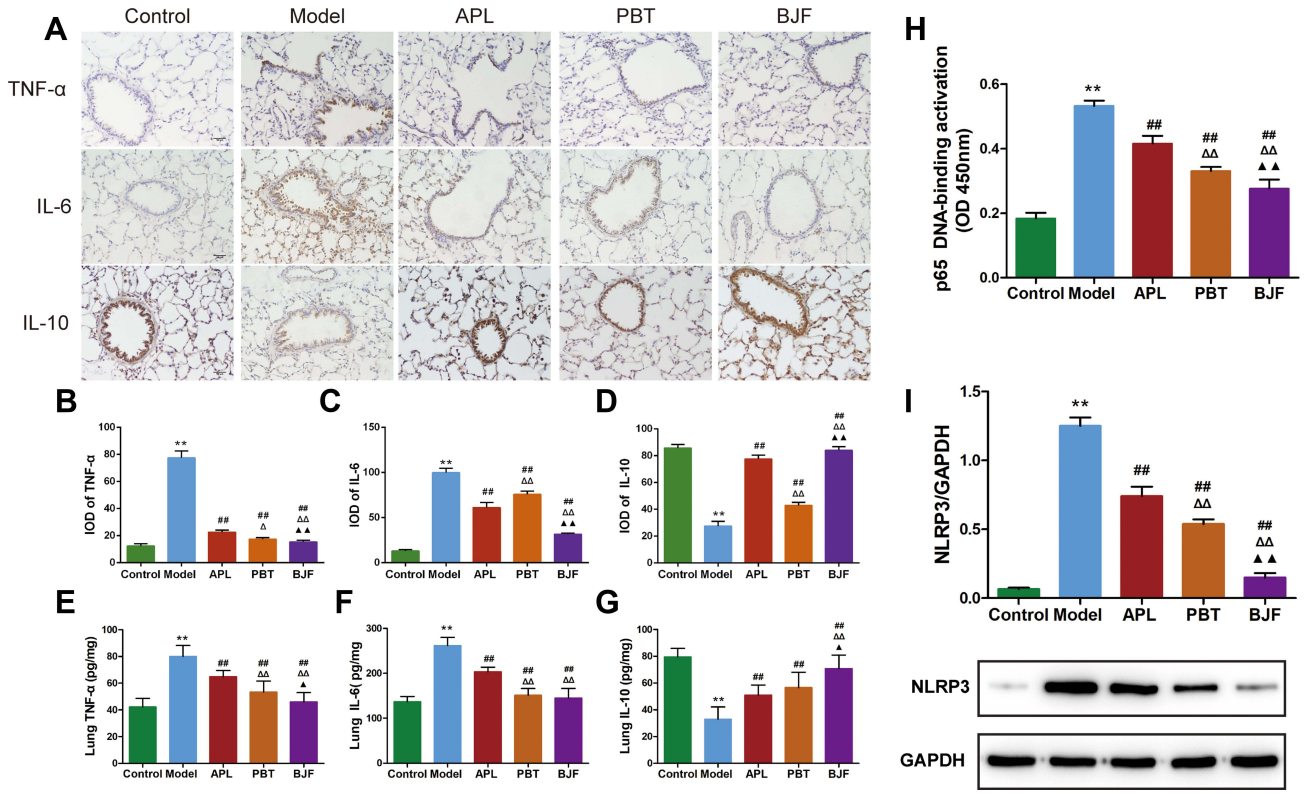

Figure 2 Effect of BJF on the Inflammatory Responses in COPD rat lung tissue. (**A**) TNF-α, IL-6 and IL-10 were detected with immunohistochemistry (magnification, ×200). (**B**–**D**) Quantitative analysis for TNF-α, IL-6 and IL-10 expression was performed. (**E**–**G**) Level of TNF-α, IL-6 and IL-10 in lung tissue. (**H**) Changes of DNA binding activity of NF-κB p65 in the lung. (**I**) The protein levels of NLRP3 in lung tissue were quantified by Western blotting. Data are presented as mean ± SD. N = 6 for each group. $^{**}p < 0.01$ vs control group; $^{\#\#}p < 0.01$ vs model group; $^{\Delta\Delta}p < 0.01$, $^{\Delta}p < 0.05$ vs aminophylline (APL) group; $^{\blacktriangle\blacktriangle}p < 0.01$, $^{\blacktriangle}p < 0.05$ vs probiotics (PBT) group.

The NF-κB signaling pathway is considered a key target in COPD development and progression. To investigate the effect of BJF on NF-κB signaling, NF-κB DNA binding activity was measured. NF-κB p65 activation was notably higher in the COPD group compared with the control; BJF, APL and PBT treatment significantly suppressed this increase (Figure 2H, $P < 0.01$).

COPD is characterized by irreversible airflow obstruction as well as airway inflammation. NLRP3 has been shown to play important roles in COPD,[19,20] so we examined lung NLRP3 protein expression to explore the effect of BJF. NLRP3 protein expression was significantly increased in the COPD rats, and markedly decreased after BJF, APL and PBT treatment (Figure 2I, $P < 0.01$). These data demonstrate that BJF treatment could alleviate pulmonary inflammatory responses in COPD rats.

Modulatory Effects of BJF on Gut Microbiota Composition in COPD Model Rats

To explore the effect of BJF on gut microbiota, 16S rRNA gene sequence analysis was performed. We obtained 3,815,197 high-quality reads and used α diversity analysis to assess the effect of BJF on the richness and diversity of the gut microbiota. Chao1 and Shannon indices were lower in the model group than in the control group (Figure 3A and B, $P < 0.05$); BJF, APL and PBT treatment reversed this change of Chao1 index (Figure 3A, $P < 0.01$), and BJF or PBT treatment increased the Shannon index (Figure 3B, $P < 0.05$). There was no significant difference in Shannon index between the Model and APL groups (Figure 3B, $P > 0.05$). We also examined the changes in gut microbiota at the phylum and genus levels. 90–97% of the gut bacterial community was composed of Firmicutes (91.50%), Bacteroides (3.02%), Proteobacteria (1.46%), Spirochaetes (1.31%), and TM7 (1.28%) in normal rats. A decreased proportion of Firmicutes and increased proportions of Bacteroides, Proteobacteria and Spirochaetes were observed in COPD rats (Figure 3C and D, $P < 0.05$). BJF treatment reversed these alterations (Figure 3C and D, $P < 0.05$), and PBT treatment moderated the increase of Proteobacteria and Spirochaetes (Figure 3C and D, $P < 0.05$). The ratio of Firmicutes to Bacteroidetes (F:B), which together make up about 94%

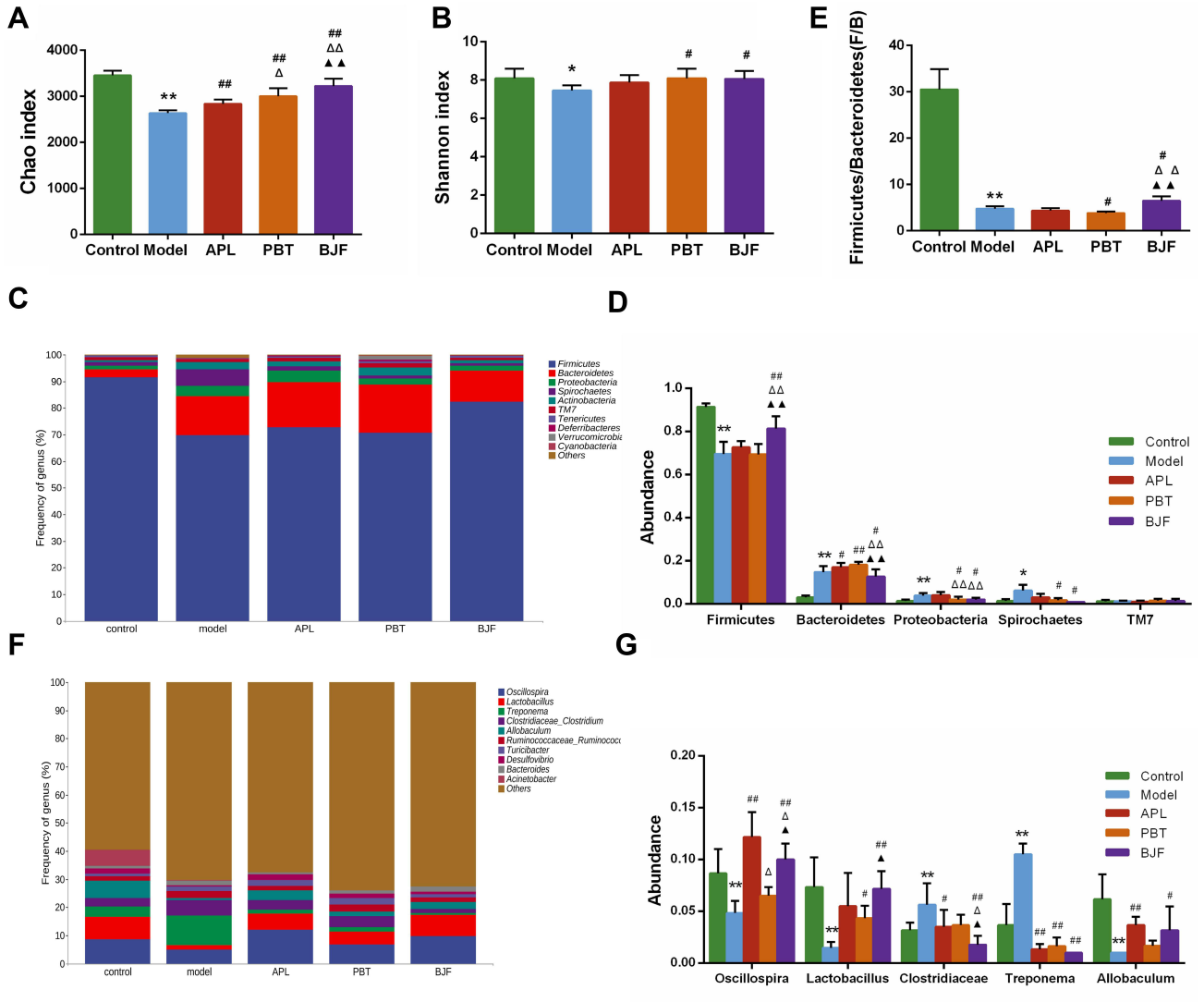

Figure 3 Modulatory effects of Bufei Jianpi Formula (BJF) on the gut microbiota composition in COPD model rats. (**A**) Chao and (**B**) Shannon diversity index. (**C**) Detailed relative abundance of the community at the phylum level. (**D**) The relative abundance of Firmicutes, Bacteroides, Proteobacteria, Spirochaetes, and TM7. (**E**) The ratio of Firmicutes/Bacteroides. (**F**) Detailed relative abundance of the community at the genus level. (**G**) The relative abundances of Oscillospira, Lactobacillus, Clostridiaceae, Treponema, and Allobaculum. Data are presented as the mean ± SD. N = 6 for each group. $^{**}p < 0.01$, $^{*}p < 0.05$ vs control group; $^{\#\#}p < 0.01$, $^{\#}p < 0.05$ vs model group; $^{\Delta\Delta}P < 0.01$, $^{\Delta}P < 0.05$ vs aminophylline (APL) group; $^{\blacktriangle\blacktriangle}p < 0.01$, $^{\blacktriangle}p < 0.05$ vs probiotics (PBT) group.

of the gut microbiota, was lower in the model group than in the control group (Figure 3E, $P < 0.01$). As expected, BJF or PBT treatment increased this ratio (Figure 3E, $P < 0.05$), suggesting that BJF and PBT regulate dysbacteriosis in COPD rats. At the genus level, Oscillospira, Lactobacillus, and Allobaculum were less abundant in the model group than in the control group. BJF treatment significantly enriched their relative abundance (Figure 3F and G, $P < 0.05$). Finally, the proportions of Clostridiaceae and Treponema were significantly elevated in COPD rats, and BJF treatment decreased their relative abundances (Figure 3F and G, $P < 0.05$). Altogether, these data indicate that BJF treatment effectively modulates gut microbiota structure in rats with COPD.

Effects of BJF on SCFA Production and Intestinal Mucosal SIgA in COPD Model Rats

To explore the effect of BJF on SCFA production, fecal SCFA levels were determined by GC/MS. In this study, the levels of SCFAs, particularly acetate, butyrate, and propionate, in the model group were significantly lower than in the control group (Figure 4A–C, $P < 0.01$). Meanwhile, BJF treatment increased the concentrations of acetate, butyrate and propionate (Figure 4A–C, $P < 0.05$), and PBT treatment significantly increased the acetate concentration (Figure 4A,

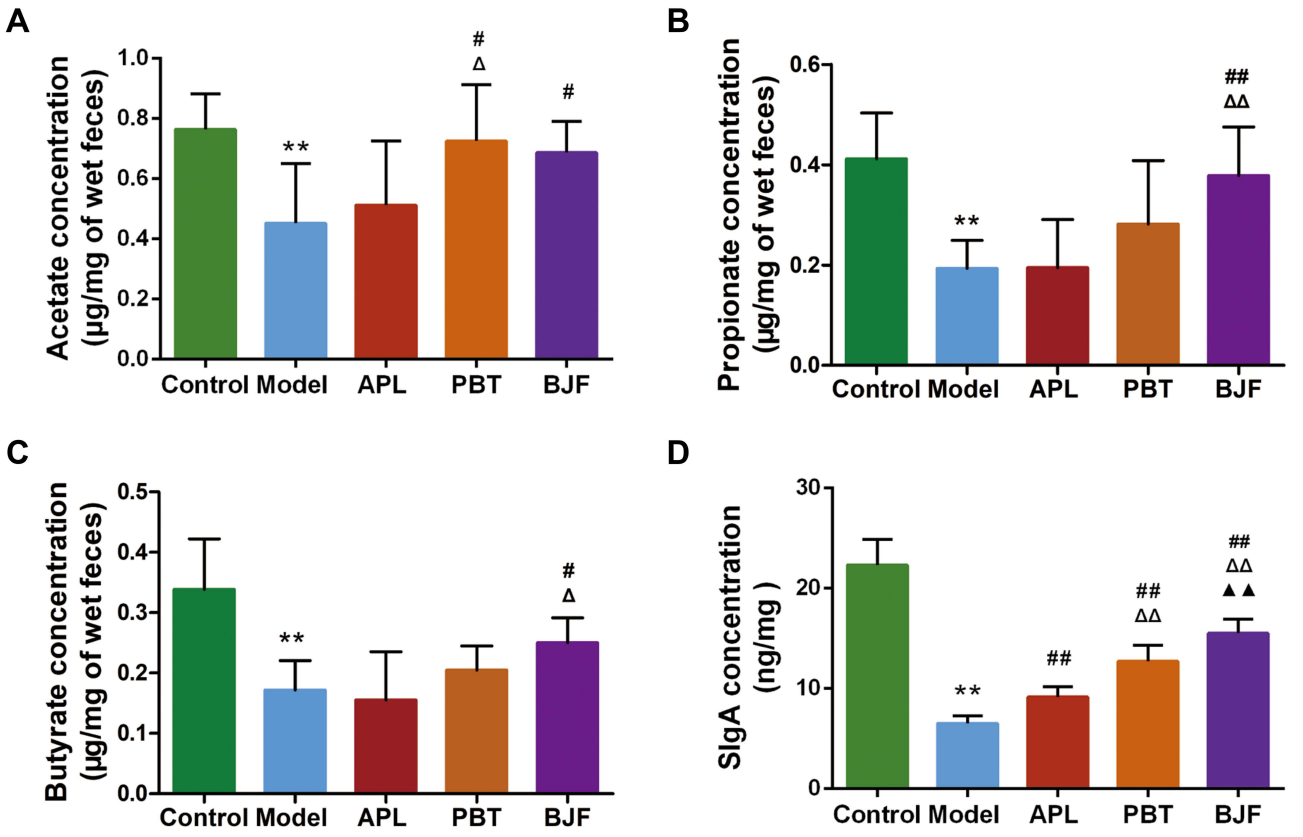

Figure 4 Effects of Bufei Jianpi Formula (BJF) on the levels of fecal SCFAs and intestinal mucosal SIgA in COPD model rats. (**A**–**C**) Acetate, propionate, and butyrate concentrations in feces. (**D**) SIgA levels in the intestinal mucosa of each group. Data are presented as the mean ± SD. N = 6 for each group. $^{**}p < 0.01$ vs control group; $^{\#\#}p < 0.01$, $^{\#}p < 0.05$ vs model group; $^{\Delta\Delta}P < 0.01$, $^{\Delta}P < 0.05$ vs aminophylline (APL) group; $^{\blacktriangle\blacktriangle}p < 0.01$ vs probiotics (PBT) group.

$P < 0.05$). Our results indicate that BJF treatment elevated the local colonic levels of SCFAs. The gut microbiota and intestinal mucosal immune system are important aspects of the gut-lung axis.

To address the role of the intestinal mucosal immune system in COPD and the therapeutic mechanism of BJF, SIgA levels in the intestinal mucosa were analyzed. SIgA expression in COPD rats was significantly lower than in the control rats (Figure 4D, $P < 0.01$). It recovered after administration of BJF, APL, or PBT, and was highest in the BJF group ($P < 0.01$).

Correlation Analysis of the Key Microbial Communities, Intestinal Mucosal Proteins, and Fecal SCFA Levels

To investigate the relationship between the key gut microbial communities, fecal SCFA levels, and intestinal mucosal proteins, Spearman correlation analysis was performed. At the phylum level, the abundance of Firmicutes, which are SCFA-producing bacteria, was positively correlated with butyrate, Propionate and SIgA (Figure 5A, $P < 0.001$). In contrast, the abundance of Bacteroidetes and Proteobacteria showed a significant negative correlation with the levels of SCFAs and SIgA (Figure 5A, $P_{propionate} < 0.05$, $P_{butyrate} < 0.001$, $P_{SIgA} < 0.001$). At the genus level, Lactobacillus, which was upregulated by BJF, was positively correlated with propionate and SIgA (Figure 5B, $P_{propionate} < 0.01$, $P_{SIgA} < 0.001$). Overall, Allobaculum showed a significant positive correlation with butyrate and SIgA levels (Figure 5B, $P_{butyrate} < 0.05$, $P_{SIgA} < 0.001$). We found that the relative abundance of the SCFA-producing Bifidobacterium was positively correlated with acetate and SIgA levels (Figure 5B, $P_{acetate} < 0.05$, $P_{SIgA} < 0.01$). Further, Clostridiaceae and Treponema, which were downregulated by BJF, were negatively associated with SIgA (Figure 5B, $P < 0.05$). These results suggest that BJF could improve the intestinal mucosal immune function of COPD rats by increasing the abundance of SCFA-producing bacteria.

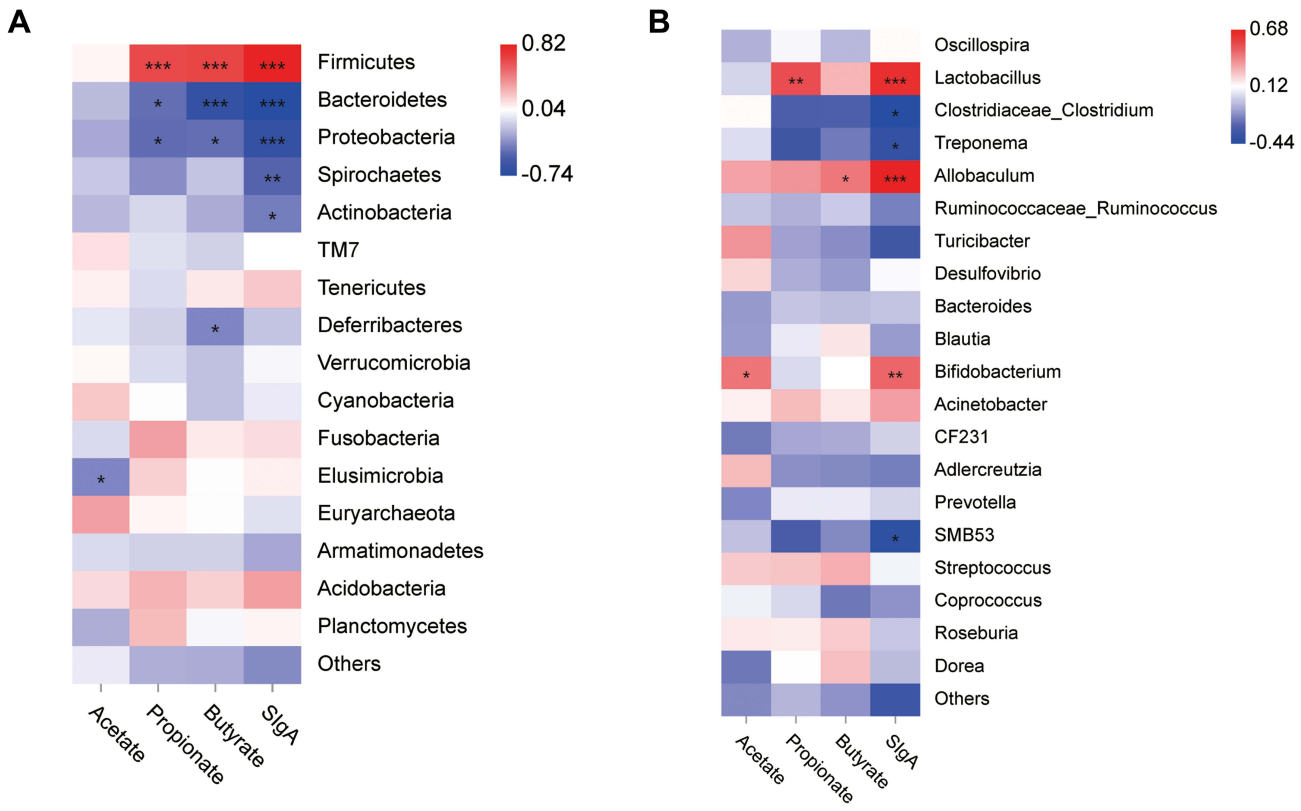

Figure 5 Heatmap of Spearman correlation between the gut microbiota [at the phylum level (**A**) and genus level (**B**)] and the intestinal mucosal protein or fecal SCFA levels. Red grids indicate positive correlations, whereas blue grids indicate negative correlations. Significant correlations are indicated by ***$p < 0.001$, **$p < 0.01$, *$p < 0.05$.

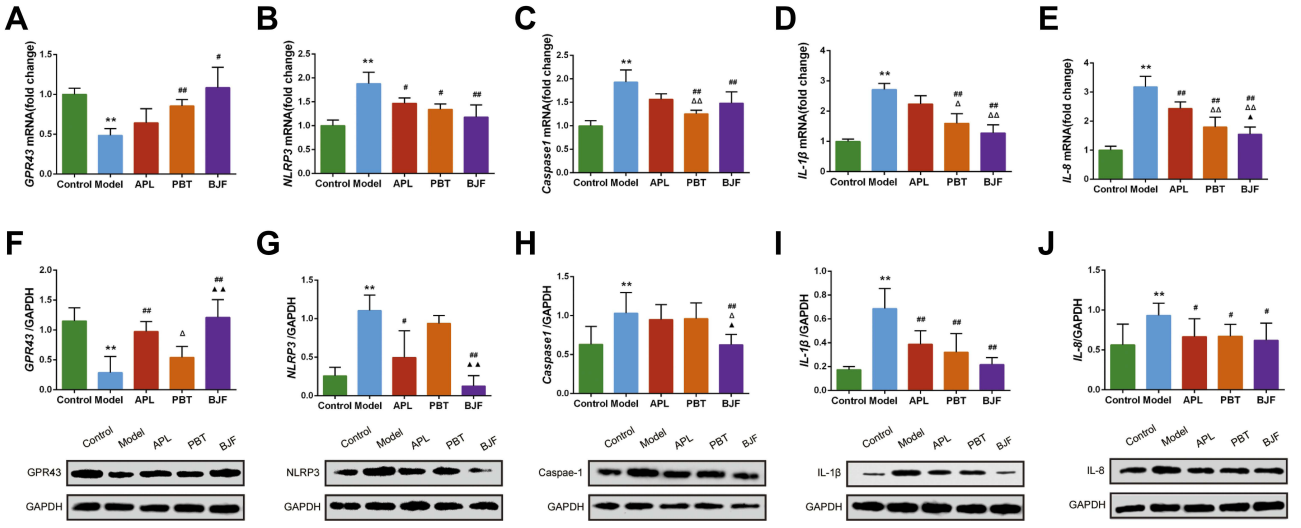

Figure 6 Effects of BJF on the SCFAs/GPR43/NLRP3 signaling pathway in COPD model rats. (**A**–**E**) The mRNA levels of GPR43, NLRP3, Caspase-1, IL-1β, and IL-8 in colon tissues were analyzed by real-time PCR. (**F**–**J**) The protein levels of GPR43, NLRP3, caspase-1, IL-1β, and IL-8 in colon tissues were quantified by Western blotting. Data are presented as mean ± SD. N = 6 for each group. **$p < 0.01$ vs control group; $^{\#\#}p < 0.01$, $^{\#}p < 0.05$ vs model group; $^{\Delta\Delta}P < 0.01$, $^{\Delta}P < 0.05$ vs aminophylline (APL) group; $^{\blacktriangle\blacktriangle}p < 0.01$, $^{\blacktriangle}p < 0.05$ vs probiotics (PBT) group.

Effects of BJF on the SCFAs/GPR43/NLRP3 Signaling Pathway in COPD Model Rats

The above results suggest that decreased levels of SCFAs could activate the intestinal mucosal response. The SCFAs/GPR43/NLRP3 pathway plays an important role in improving the intestinal mucosal responses. To further explore the effects of BJF treatment on the SCFAs/GPR43/NLRP3 signaling pathway, the gene and protein expressions of GPR43, NLRP3, Caspase-1, IL-8, and IL-1β were analyzed. GPR43 mRNA expression was lower in the model group than in the control group (Figure 6A, $P < 0.01$). BJF and PBT treatment increased it, especially in the BJF group (Figure 6A, $P < 0.05$). Consistently, the mRNA expression levels of NLRP3, Caspase-1, IL-8, and IL-1β were significantly upregulated in COPD rats compared with the control group. However, BJF or PBT treatment produced a remarkable decrease (Figure 6B–E, $P < 0.05$, $P < 0.01$). Similarly, BJF increased GPR43 protein expression and inhibited those of its downstream genes, including NLRP3, Caspase-1, IL-8, and IL-1β (Figure 6F–J, $P < 0.05$). Including these data, the results indicate that BJF could improve intestinal mucosal response via the SCFAs/GPR43/NLRP signaling pathway.

Discussion

Traditional Chinese medicine theories suggest that the main syndrome of the stable phase of COPD is caused by lung and spleen qi deficiency.[21] Therefore, BJF has been developed based on the principle of "strengthening the spleen, tonifying the lung, and reinforcing the earth to generate the metal" as a prescription against the disease. The evaluation index of the COPD rat model included pulmonary function decline and representative lung pathological impairments. FEV1 and FEV1/FVC are critical for evaluating lung function in COPD. The Global Initiative for Chronic Obstructive Lung Disease (GOLD) guidelines indicate that FEV1 is associated with severity of COPD. Consistent with clinical COPD, the changes of FEV0.3/FVC in COPD rats showed that lung function was damaged. And the lung damage was rescued by BJF treatment. We also found marked inflammatory cell infiltration, bronchiolar stenosis, and alveolar expansion and destruction in the COPD rats, which were improved in the treated groups. Inflammation is central to the development of COPD, which involves the infiltration of the major inflammatory cells, including neutrophils, monocytes/macrophages, and lymphocytes, into the airway and lung tissue.[22] In this study, the levels of inflammatory factors (IL-6, TNF-α and IL-10) in lung tissue were noticeably changed, implying that the degree of inflammation was increased in the lungs of COPD rats. The inflammatory reaction was effectively repressed by BJF treatment.

A growing number of studies have demonstrated that CSE or Bacterial infection is able to activate NF-κB through toll-like receptors, resulting in the production of proinflammatory cytokines including TNF-α, IL-1β, and IL-6.[23] NF-κB also serves as the priming signal to facilitate the transcriptional expression of NLRP3 and pro-IL-1β.[24] Our results also show that the expression of NLRP3 and NF-κB activity is remarkably enhanced in the lung tissues of COPD rats. The BJF treatment significantly inhibited these expressions. We speculate that these changes might partly explain BJF's contribution to alleviating the lung inflammatory response during COPD. These data taken together show that BJF has a positive therapeutic effect on COPD, which is consistent with previous findings.[17]

Recently, a certain pathophysiological correlation between the respiratory and gastrointestinal tracts, the mutual influence of which is exhibited through the gut-lung axis.[25,26] Studies have reported that gut mucosal immunity affects the immune response of the lung, wherein the gut microbiome promotes COPD initiation and development through mucosal immunity.[27] In addition, most COPD patients have a long history of smoking. Studies have indicated that chronic smoke exposure can alter the structure of gut microbes, which alters the gut microbiome and is associated with the incidence of acute COPD.[28] Lachnospiraceae sp. were reported to be increased in the mouse gut after smoke exposure.[29] Therefore, in this study, the abundance of the gut microbiome was measured to understand its role in COPD. Our results showed that the gut microbiome was highly diversified and abundant in control rats, with Firmicutes, Bacteroidetes, and Proteobacteria being the most abundant intestinal bacteria. In contrast, among COPD rats, the α-diversity was substantially changed, with decreased levels of Firmicutes, Oscillospira, and Lactobacillus, and increased levels of Clostridiaceae, consistent with the available literature.[30] However, the gut microbiomes are somewhat different in the previous studies.[14] An experimental factor that the duration and intensity of the CSE may explain the discordant findings during the acute exacerbation and stable phase of COPD.

Previous studies have shown that F:B is a predictor of fecal SCFA levels, as these two clades, along with Laospirillaceae, include important symbiotic, SFCA-producing bacteria.[31,32] In our study, a decrease in the F:B ratio was observed among COPD rats, indicating that alterations in the gut microbiome, especially reduction of SCFA-producing bacteria, could lead to the initiation and development of COPD. SCFA has been established as a mediator of the gut-lung axis. As BJF considerably increased the abundance of SCFA-producing bacteria, the intestinal immune barrier was strengthened, thereby protecting the mucosal immune system and alleviating COPD. Therefore, homeostatic maintenance of the gut microbiome may be a viable treatment strategy for COPD.

As important beneficial metabolites of the gut microbiome, SCFAs including acetate, butyrate, and propionate, are the primary energy source of intestinal mucosal cells.[33] Moreover, both the human respiratory and gastrointestinal tracts can produce SIgA, which acts as the main mediator of mucosal immunity. In particular, SIgA is connected through homing migration and the common immune system, serving as an important basis for the correlation between the lungs and large intestine.[34] The present study revealed that compared to healthy rats, the SCFA and SIgA levels in the gut mucosa of COPD rats were substantially lower, indicating compromised intestinal mucosal immune function. To further verify the relationship between the gut microbiome and mucosal immunity, a correlation analysis was performed. Notably, the results indicated that among different SCFA-producing bacteria, the relative abundance of Firmicutes was positively correlated with SIgA and SCFA levels, whereas the relative abundance of Bacteroidetes and Proteobacteria was negatively correlated. Alternatively, at the genus level, the relative abundance of the SCFA-producing Bifidobacterium was positively correlated with SIgA levels. Thus, we speculated that BJF could improve the intestinal mucosal immune function of COPD rats by increasing the abundance of SCFA-producing bacteria.

To further clarify the molecular mechanism of BJF in regulating the gut microbiome of COPD rats, we also investigated the expression of inflammasome pathways. Several studies have indicated that as the most important molecular mechanism for maintaining intestinal epithelial integrity and gut homeostasis, these inflammasome pathways regulate changes in Escherichia coli in the gut microbiome through IL-18.[35] Furthermore, IL-1β is an important component of cigarette smoke-induced inflammation and COPD.[36] The NLRP3 inflammasome is upregulated in COPD and COPD exacerbation in vitro.[37] In this study, we found that BJF upregulated GPR43 expression and downregulated NLRP3, caspase-1, IL-1β, and IL-18 expression in COPD rats. These results suggest that BJF can improve gut microbiome alterations and gut metabolome changes by regulating the intestinal SCFAs/GPR43/NLRP3 pathway, thereby enhancing gut mucosal immune function.

There are some limitations in this study. Firstly, because of the intimate relationship between the respiratory and gastrointestinal tract, further work should focus on whether the changes in gut and lung microbiota composition are consistent. In addition, future studies are needed to determine the most effective ingredients for treatment.

Conclusion

In conclusion, these results demonstrate that BJF can improve mucosal immune function by remodeling the gut microbiota and modulating metabolites through suppression of the SCFAs/GPR43/NLRP3 pathway in COPD rats. This evidence supports the clinical application of BJF in COPD treatment.

Abbreviations

COPD, chronic obstructive pulmonary disease; BFJ, Bufei Jianpi formula; SD, Sprague–Dawley; APL, aminophylline; PBT, probiotics; LPS, lipopolysaccharide; CSE, cigarette smoke extract; GC, gas chromatography; MS, mass spectrometry; SCFAs, short-chain fatty acids; APS, Astragalus polysaccharides; FVC, forced expiratory vital capacity; FEV0.3, forced expiratory volume in 0.3 s; H&E, hematoxylin and eosin; PAS, Periodic Acid-Schi; SIgA, secretory IgA; MTBE, methyl tert-butyl ether; SDS-PAGE, sodium dodecyl sulfate polyacrylamide gel electrophoresis; PVDF, polyvinylidene difluoride; ANOVA, one-way analysis of variance; SD, standard deviation.

Data Sharing Statement

The raw data supporting the conclusions of this article will be made available by the authors, without undue reservation, to any qualified researcher.

Ethics Approval

All animal studies were approved by the Animal Ethics Committee of Henan University of Chinese Medicine (DWLL2019020002) and performed according to the guidelines of the Henan University of Chinese Medicine Animal Care and Use Committee.

Funding

This research was supported by the National Natural Science Fund of China (No. 81904116), Chinese Medicine inheritance and innovation "thousand million" Talents Project (Qihuang Project) Qihuang Scholars (No. [2018]284), and the Scientific Research Fund for doctors of Henan University of Chinese Medicine (No. RSBSJJ2018-03).

Disclosure

The authors report no conflicts of interest in relation to this work and declare that the research was conducted in the absence of any commercial or financial relationships that could be construed as a potential conflict of interest.

References

1. Moraga P. Global, regional, and national age-sex specific mortality for 264 causes of death, 1980–2016: a systematic analysis for the Global Burden of Disease Study 2016. *Lancet*. 2017;390(10100):1151–1210. doi:10.1016/s0140-6736(17)32152-9
2. World Health Organization. Mortality and global health estimates. Available from: http://who.int/data/gho/data/themes/mortality-and-global-health-estimates. Accessed November 21, 2020.
3. Vaughan A, Frazer ZA, Hansbro PM, Yang IA. COPD and the gut-lung axis: the therapeutic potential of fibre. *J Thorac Dis*. 2019;11(Suppl 17):S2173–S2180. doi:10.21037/jtd.2019.10.40
4. Budden KF, Gellatly SL, Wood DL, et al. Emerging pathogenic links between microbiota and the gut-lung axis. *Nat Rev Microbiol*. 2017;15(1):55–63. doi:10.1038/nrmicro.2016.142
5. Bowerman KL, Rehman SF, Vaughan A, et al. Disease-associated gut microbiome and metabolome changes in patients with chronic obstructive pulmonary disease. *Nat Commun*. 2020;11(1):5886. doi:10.1038/s41467-020-19701-0
6. Marsland BJ, Trompette A, Gollwitzer ES. The gut-lung axis in respiratory disease. *Ann Am Thorac Soc*. 2015;12(Suppl 2):S150–S156. doi:10.1513/AnnalsATS.201503-133AW
7. Hand TW, Vujkovic-Cvijin I, Ridaura VK, Belkaid Y. Linking the microbiota, chronic disease, and the immune system. *Trends Endocrinol Metab*. 2016;27(12):831–843. doi:10.1016/j.tem.2016.08.003
8. He Y, Wen Q, Yao F, Xu D, Huang Y, Wang J. Gut-lung axis: the microbial contributions and clinical implications. *Crit Rev Microbiol*. 2017;43(1):81–95. doi:10.1080/1040841X.2016.1176988
9. Macia L, Tan J, Vieira AT, et al. Metabolite-sensing receptors GPR43 and GPR109A facilitate dietary fibre-induced gut homeostasis through regulation of the inflammasome. *Nat Commun*. 2015;6(1):6734. doi:10.1038/ncomms7734
10. Fujiwara H, Docampo MD, Riwes M, et al. Microbial metabolite sensor GPR43 controls severity of experimental GVHD. *Nat Commun*. 2018;9(1):3674. doi:10.1038/s41467-018-06048-w
11. Hong Y, Li B, Zheng N, et al. Integrated metagenomic and metabolomic analyses of the effect of astragalus polysaccharides on alleviating high-fat diet-induced metabolic disorders. *Front Pharmacol*. 2020;11:833. doi:10.3389/fphar.2020.00833
12. Zhao P, Li J, Li Y, et al. Systems pharmacology-based approach for dissecting the active ingredients and potential targets of the Chinese herbal Bufei Jianpi formula for the treatment of COPD. *Int J Chron Obstruct Pulmon Dis*. 2015;10:2633–2656. doi:10.2147/COPD.S94043
13. Dong Y, Li Y, Sun Y, et al. Bufei Jianpi granules improve skeletal muscle and mitochondrial dysfunction in rats with chronic obstructive pulmonary disease. *BMC Complement Altern Med*. 2015;15(1):51. doi:10.1186/s12906-015-0559-x
14. Li X, Li Y, Mao J, et al. Combination of Chinese and Western medicine optimizes the intestinal microbiota of exacerbated chronic obstructive pulmonary disease in rats. *Evid Based Complement Alternat Med*. 2021;2021:9975407. doi:10.1155/2021/9975407
15. Zhang XF, Zhu J, Geng WY, et al. Electroacupuncture at Feishu (BL13) and Zusanli (ST36) down-regulates the expression of orexins and their receptors in rats with chronic obstructive pulmonary disease. *J Integr Med*. 2014;12(5):417–424. doi:10.1016/S2095-4964(14)60040-6
16. Li Y, Li JS, Li WW, et al. Long-term effects of three Tiao-Bu Fei-Shen therapies on NF-kappaB/TGF-beta1/smad2 signaling in rats with chronic obstructive pulmonary disease. *BMC Complement Altern Med*. 2014;14:140. doi:10.1186/1472-6882-14-140
17. Mao J, Li Y, Feng S, et al. Bufei Jianpi formula improves mitochondrial function and suppresses mitophagy in skeletal muscle via the adenosine monophosphate-activated protein Kinase pathway in chronic obstructive pulmonary disease. *Front Pharmacol*. 2020;11:587176. doi:10.3389/fphar.2020.587176
18. Huang F, Zheng X, Ma X, et al. Theabrownin from Pu-erh tea attenuates hypercholesterolemia via modulation of gut microbiota and bile acid metabolism. *Nat Commun*. 2019;10(1):4971. doi:10.1038/s41467-019-12896-x
19. Tian X, Xue Y, Xie G, et al. (-)-Epicatechin ameliorates cigarette smoke-induced lung inflammation via inhibiting ROS/NLRP3 inflammasome pathway in rats with COPD. *Toxicol Appl Pharmacol*. 2021;429:115674. doi:10.1016/j.taap.2021.115674
20. Zhang MY, Jiang YX, Yang YC, et al. Cigarette smoke extract induces pyroptosis in human bronchial epithelial cells through the ROS/NLRP3/caspase-1 pathway. *Life Sci*. 2021;269:119090. doi:10.1016/j.lfs.2021.119090
21. Zhi ZYZ. Syndrome diagnostic criteria of traditional Chinese medicine for chronic obstructive pulmonary disease; 2011:177–178.
22. Wang Y, Xu J, Meng Y, et al. Role of inflammatory cells in airway remodeling in COPD. *Int J Chron Obstruct Pulmon Dis*. 2018;13:3341–3348. doi:10.2147/COPD.S176122
23. Liu T, Zhang L, Joo D, et al. NF-κB signaling in inflammation. *Signal Transduct Target Ther*. 2017;2(1):17023. doi:10.1038/sigtrans.2017.23

24. Zhao C, Zhao W. NLRP3 inflammasome-A key player in antiviral responses. *Front Immunol*. 2020;11:211. doi:10.3389/fimmu.2020.00211
25. Tan JY, Tang YC, Huang J. Gut Microbiota and Lung Injury. *Adv Exp Med Biol*. 2020;1238:55–72. doi:10.1007/978-981-15-2385-4-5
26. Chunxi L, Haiyue L, Yanxia L, Jianbing P, Jin S. The gut microbiota and respiratory diseases: new evidence. *J Immunol Res*. 2020;2020:2340670. doi:10.1155/2020/2340670
27. Lee SH, Yun Y, Kim SJ, et al. Association between cigarette smoking status and composition of gut microbiota: population-based cross-sectional study. *J Clin Med*. 2018;7(9):282. doi:10.3390/jcm7090282
28. Biedermann L, Zeitz J, Mwinyi J, et al. Smoking cessation induces profound changes in the composition of the intestinal microbiota in humans. *PLoS One*. 2013;8(3):e59260. doi:10.1371/journal.pone.0059260
29. Allais L, Kerckhof FM, Verschuere S, et al. Chronic cigarette smoke exposure induces microbial and inflammatory shifts and mucin changes in the murine gut. *Environ Microbiol*. 2016;18(5):1352–1363. doi:10.1111/1462-2920.12934
30. Fernandes J, Su W, Rahat-Rozenbloom S, et al. Adiposity, gut microbiota and faecal short chain fatty acids are linked in adult humans. *Nutr Diabetes*. 2014;4:e121. doi:10.1038/nutd.2014.23
31. Wang Y, Li N, Li Q, et al. Xuanbai Chengqi decoction ameliorates pulmonary inflammation via reshaping gut microbiota and rectifying Th17/Treg imbalance in a murine model of chronic obstructive pulmonary disease. *Int J Chron Obstruct Pulmon Dis*. 2021;16:3317–3335. doi:10.2147/COPD.S337181
32. Ji J, Ge X, Chen Y, et al. Daphnetin ameliorates experimental colitis by modulating microbiota composition and Treg/Th17 balance. *FASEB J*. 2019;33(8):9308–9322. doi:10.1096/fj.201802659RR
33. Yang H, Duan Z. The local defender and functional mediator: gut microbiome. *Digestion*. 2018;97(2):137–145. doi:10.1159/000484687
34. Anand S, Mande SS. Diet, microbiota and gut-lung connection. *Front Microbiol*. 2018;9:2147. doi:10.3389/fmicb.2018.02147
35. Donovan C, Liu G, Shen S, et al. The role of the microbiome and the NLRP3 inflammasome in the gut and lung. *J Leukoc Biol*. 2020;108 (3):925–935. doi:10.1002/JLB.3MR0720-472RR
36. Man SM. Inflammasomes in the gastrointestinal tract: infection, cancer and gut microbiota homeostasis. *Nat Rev Gastroenterol Hepatol*. 2018;15 (12):721–737. doi:10.1038/s41575-018-0054-1
37. Nachmias N, Langier S, Brzezinski RY, et al. NLRP3 inflammasome activity is upregulated in an in-vitro model of COPD exacerbation. *PLoS One*. 2019;14(5):e0214622. doi:10.1371/journal.pone.0214622